AENSI Journals
Advances in Environmental Biology
ISSN:1995-0756 EISSN: 1998-1066
Journal home page: http://www.aensiweb.com/aeb.html

Investigation on The Effect of Ultrasound Waves on Stainless Steel Surfaces During Removal of Soil Films

[1]T.A.Mamvura, [1]S.E.Iyuke, [1]A.E. Paterson

[1]*School of Chemical and Metallurgical Engineering, Faculty of Engineering and the Built Environment, University of the Witwatersrand, Wits 2050, Johannesburg, South Africa.*

ARTICLE INFO

Article history:
Received 14 Feb 2014
Received in revised form 24 February 2014
Accepted 29 March 2014
Available online 14 April 2014

Key words:
Ultrasound waves, welding, surface erosion, atomic force microscopy

ABSTRACT

The purpose of this study was to investigate the effect of using ultrasound waves at 24 kHz on surface topography of three stainless steel coupons during soil film removal. Atomic force microscopy (AFM), a major discovery as a non-destructive analysis tool was used in the analysis of surface topography and morphology in non-contact (tapping) mode. Coupons before and after treatment with ultrasound waves (after 9 adhesion-cleaning cycles) were used and quantified in the study. Quantitative measurements according to topographic and morphological parameters: average roughness (R_a), root-mean-square profile height (R_q), maximum peak-to-valley height(R_{max}), surface skewness(R_{skw}) and surface kurtosis (R_{kur}) were studied on ($7x5cm^2$) coupons for AFM scanning area of $25x25\mu m^2$. The results revealed that normal surfaces (surfaces not welded) had pits/valleys which were good lubrication whilst welding (heat treatment) processes modified the surface by introducing peaks resulting in rougher surfaces and increased soil film intensity. After treatment with ultrasound waves to remove soil films, there was considerable flattening of the surfaces i.e. erosion of peaks (more pronounced on welds) giving smoother surfaces that discourage soil film growth. The data was confirmed by topography and morphological data presented.

To Cite This Article: TA Mamvura, SE Iyuke, AE Paterson., Investigation on the effect of ultrasound waves on stainless steel surfaces during removal of soil films. ***Adv. Environ. Biol., 8(3),*** *572-581, 2014*

INTRODUCTION

General introduction:

Austenitic stainless steels have been used in various components and facilities of the food and beverage industries because of their excellent corrosion resistance and ease of cleanability. Welding processes are used to join pipeworks together which are then used in the beverage industries. However, weld regions are particularly attractive to microbes as the welding process alters the material surface characteristics. Adhesion of bacteria to stainless steel surfaces in aqueous media or humid environments is the initial step in the formation of soil films which are known to cause problems such as microbiologically influenced corrosion (MIC) or they represent a chronic source of microbial contamination [1,2]. As the microorganisms grow on substratum surfaces, theyproduce various metabolic by-products, which can promote deterioration of the underlying substratum. These reactions are referred to as biocorrosion or MIC when the underlying substratum is a metal or metal alloy like stainless steel. The magnitude of the problem of MIC necessitates a wider attention that might encompass collaboration between established research groups or laboratories specialising researches on various aspects of metal microbe interactions viz. microbiology, metallurgy, civil & environmental engineering and biotechnology.

Atomic force microscopy (AFM) has today become an essential tool to study surface structures down to atomic scale that can encourage soil film formation on stainless steel surfaces; and studies have led to the conclusion that rough stainless steel surfaces are more prone to corrosion which can lead to the apparition of pitting and crevices, increasing the adhesion possibilities of the microorganisms and decreasing the cleanability of the surface [3].

Effect of welding:

The combination of physical and compositional changes brought about by the welding process is believed to facilitate accumulation of organics onto the surface and subsequent colonisation by bacteria to form soil films. The preference of weld as a site of colonisation by bacteria is evident and has been correlated to the surface roughness. Welding is characterised by three effects [i] heat affected zone (HAZ), (ii) geometric effects

Corresponding Author: TA Mamvura, School of Chemical and Metallurgical Engineering, Faculty of Engineering and the Built Environment, University of the Witwatersrand, Wits 2050, Johannesburg, South Africa

(iii) filler composition used i.e. same as material composition or different. If the filler composition is different it may results in galvanic cells on the weld surface.

Incorrect welding may lead to poor hygiene conditions in an otherwise hygienically well designed plant. Thus, a residual oxygen content of more than 1% in the backing gas will lead to irregularities and burrs in the actual welding surface. Similarly, an initiating corrosion pocket may cause bacterial concentration pockets long before the actual corrosion is detected. Root defects in the welds must be avoided as they can lead to bacterial pockets. The normal roughness of a well-performed weld will be approximately 1.6 – 4 μm. The maximum roughness accepted on the product side is 6 μm. Whilst the welded area constitutes a very small part of the total area of the installation, corrosion supporting local bacterial soil film concentration and potential collapse can significantly affect bacteria counts and impact on capital equipment life.

Sensitisation resultswhen carbon in steel diffuses to the grain boundaries in the sensitised regions and it is also caused by segregation of impurities such as sulphur and phosphorus onto grain boundaries. The process occurs due to heat input during welding process and it promotes acceleration of localised attack leading to failure due to inter-granular failure [4].

Frequency and thermal stress on stainless steel surfaces:

When a bubble collapses near the surface, it yields a micro-jetwhich impinges on the surface causing either erosion or fracture andwhen the cavity rebounds, it produces a shock wave which adds to this erosion. However, in both cases the elastic limit of the solid is crossed and erosion occurs in the plastic regime [5].The impact of a micro-jet formed at the moment of a cavity collapse has a major role in causing erosion on neighbouring solid materials asthis can lead to stress waves being generated on the stainless steel when collapse impingement acts on its surface resulting in material damage [6]. However, the magnitude of the shearing stress will decrease with distance from the impacting point i.e. if bubble implosion occurs at a distance from the surfaces [6]. The frequency stress generated has an effect on the internal structure of the stainless steel and it facilitates formation of soil films. Pitting and fracture can also activate the surface by physically dislodging any passivating layer leading to increase in corrosion rates at these sites [5].

Thermal stresses are formed as a result of thermal processes, such as welding and they cause non-uniform temperature changes in materials [7]. Associated local heating, expansion and contraction because of high heat and sometimes rapid cooling occur around the heat affected zone of the material but the expansion zone is only surrounded by the material that has not been heated and this part prevents material from expanding or contracting freely leading to residual stresses[7] that modify grains and grain boundaries thereby facilitating formation of soil films. During welding, mixing of molten filler and the base metal results in a uniform chemical composition on the boundary and this becomes a weak spot[4]. Welding of 316L stainless steel results in inter-dendritic structure being formed and this area is prone to corrosionattack. Failure ofstainless steel particularly on weld zone is believed to be due to inter-dendritic attack ofinter-dendriticstructure[4].

Ultrasound waves:

Ultrasound waves are able to deagglomerate and inactivate soil films formed on stainless steel surfaces through physical, mechanical and chemical effects arising from acoustic cavitation that enhance biocide efficiency, however, this process alone does not provide powerful (100%) disinfection [8,9]. Ultrasound waves are sound waves with a frequency higher than the upper limit of human hearing of 20 kHz. The oscillatory motion due to ultrasound waves causes molecular density and pressure anisotropies to form leading to cavitation thereby destroying soil films[10,11]. In the vicinity of weak spots in the molecular lattice (i.e. imperfections in the liquid continuum caused by gas pockets, micelles, particles, and crevices in container walls) this process can generate microcavities in the solution[10, 12] that leads to cavitation. Cavitation is the formation and subsequent dynamic life of bubbles in liquids subjected to a sufficiently low pressure [13].

The undulations and craters that can be observed during use of ultrasound waves are as a result of plastic deformations which can increase the surface roughness, and they are considered as the main damage style at the incubation stage [6]. Total residual stress will increase around the weld zone, however, in the weld start and end points total residual stress is higher than at the centre of the weld [7]. Figure 1 shows a schematic of surface erosion with change in time on a surface subjected to ultrasound waves.

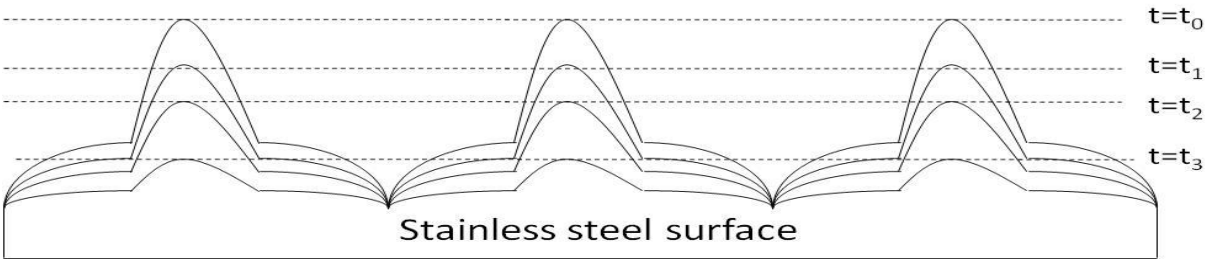

Fig. 1: Surface erosion of stainless steel subjected to ultrasound waves with time

It can be seen that ultrasound waves erode the surface of the stainless steel equally along the whole surface. However, cavitation which results in surface erosion is an uncontrolled process and sometimes it erodes the surface unevenly.

Surface profile of stainless steel:

Surfaces used in the food and beverage industry should normally have R_a< 800 nm although, values up to 3200nm would be acceptable as long as the cleaning fluid flowrate during clean-in-place is sufficient enough to remove soil films from the surfaces [14,15,16]. However, Detry*et al*[3] concluded that rough stainless steel surfaces are characterised by R_a> 500nm. The surface morphology of the stainless steel surfaces used in the beverage industryis mainly attributed to mechanical and chemical polishing processes [17].

This study described herein was aimed at investigating the effect that ultrasound waves have on stainless steelsurfaces caused by cavitation experienced during removal of soil films. The method involved subjecting ultrasound waves to stainless steel coupon surfaces with soil films attached using ultrasound waves of 24 kHz and analyse surface erosion, if any, using AFM before and after the experiments.

Experimental:

Stainless steel coupon preparation:

To simulate stainless-steel surfaces that may be encountered in a food-processing environment, food-grade stainless-steel coupons (AISI 316L stainless steel)with 3 different types of welds{Laser, cold metal transfer (CMT) and gas tungsten arc welding (GTAW), also known as tungsten inert gas (TIG) welding or gas metal arc welding (GMAW), also known as metal inert gas (MIG) welding or metal active gas (MAG) welding} were obtained from Falcon Engineering, South Africa and welded at South African Institute of Welding(SAIW). All coupons were rectangular (on average 30×22cm^2)and mechanically polished giving the same surface finish.Smooth surfaces are used in the food industry on the premise that surface polishing provides a more cleanable surface which reduces soil film formation[18].Before soil film adhesion and treatment, all coupons were cleaned with acetone to remove grease, etched with hydrochloric acid for a few minutes, individually rinsed in distilled water, allowed to air-dry under a laminar hood, and then autoclaved at 121 °C for 20 minutes[17].

Determination of surface roughness of stainless steel coupons:

Stainless steel coupons used during the experimentswere cleaned with 95% ethanol solution to remove any residuesprior to roughness measurements[19]. The topography of the coupon surfaces was quantified as surface roughnessdetermined from sixsuccessive measuring lengths.The measurements were quantified using topographic and morphological parameters:Average roughness (R_a), Root-mean-square profile height (R_q), Maximum peak-to-valley height(R_{max}),Surface skewness(R_{skw}) and Surface kurtosis (R_{kur}). The roughness parameters used are defined in Appendix I.Three parameters R_a, $R_q$and R_{max}were utilised to evaluate the coupon's surface topography, while R_{skw} and R_{kur} were used to describe the surface morphology [20]. The analysis was done on the normal surface and the three different welds available and comparison was done against the normal surface as the original surface available at the start of the study.

Atomic Force Microscopy:

Dimension 3100AFMusing Nanoscope version 5.30was used to view coupon surfaces before andafter experiments. The images of stainless steel surfaces were obtained in noncontact(tapping) mode usingstandard cantilevers. AFM is a scanning probe microscopy that allows obtaining precise three-dimensional(3D) topography of the object surface and geometrical parameters of the elements with a subnanometer resolutionfor a scanning area of 25x25μm^2. All measurements were done in ambient environment at the room temperature with AFM images processed with Nanoscope v.5.30 software and Nanotec Windows Scanning X (Force, Tunneling, and Near Optical) Microscope (WSxM) v.5.1 software[21].

Optical Microscope:

These were used initially to view the surfaces produced after welding and compared to the normal surface available initially. The microscopes used were Carl ZeissSteREO Discovery microscope.V12(Germany) and Leica DM6000M microscope(country)

RESULTS AND DISCUSSION

Changes in surface topography:

The results for surface topography and surface morphology for normal surface, back surface, front and back welded surfaces are presented in the section.

Surface profile of different surfaces used:

Surface profile for the four surfacesused in the study (normal surface, laser, CMT and MIG weld surfaces) were analysed before being used in the experiments and results are presented below:

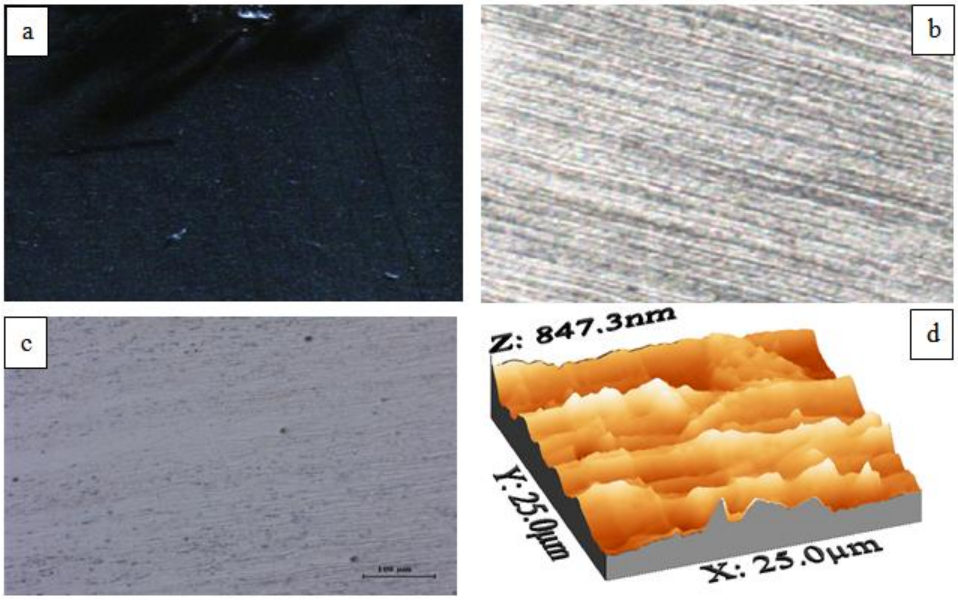

Fig. 2: Surface analysis for normal surface. (a) 5x (b) 50x (c) 200x (d) AFM for 25x25µm^2 surface area

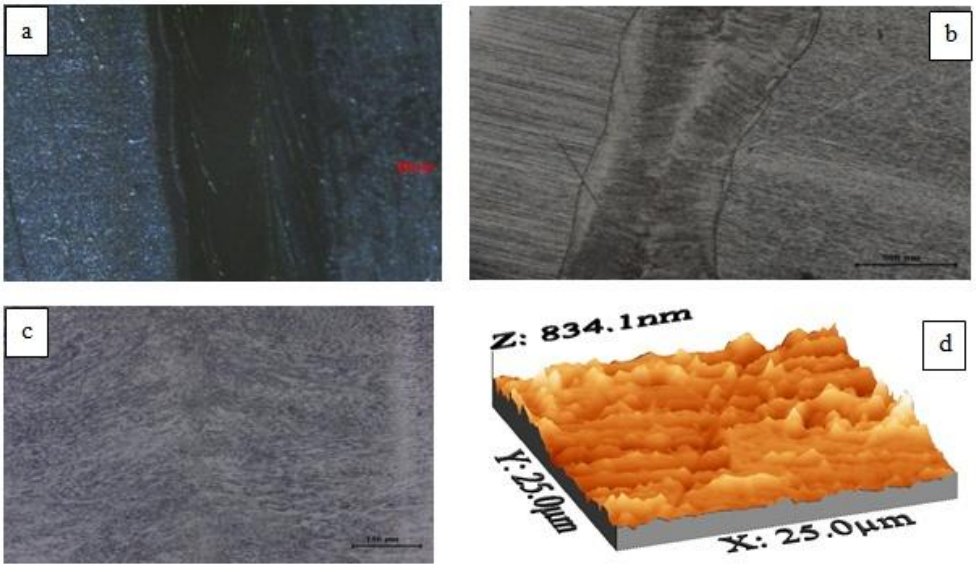

Fig. 3: Surface analysis for laser weld surface. (a) 5x (b) 50x (c) 200x (d) AFM for 25x25µm^2 surface area

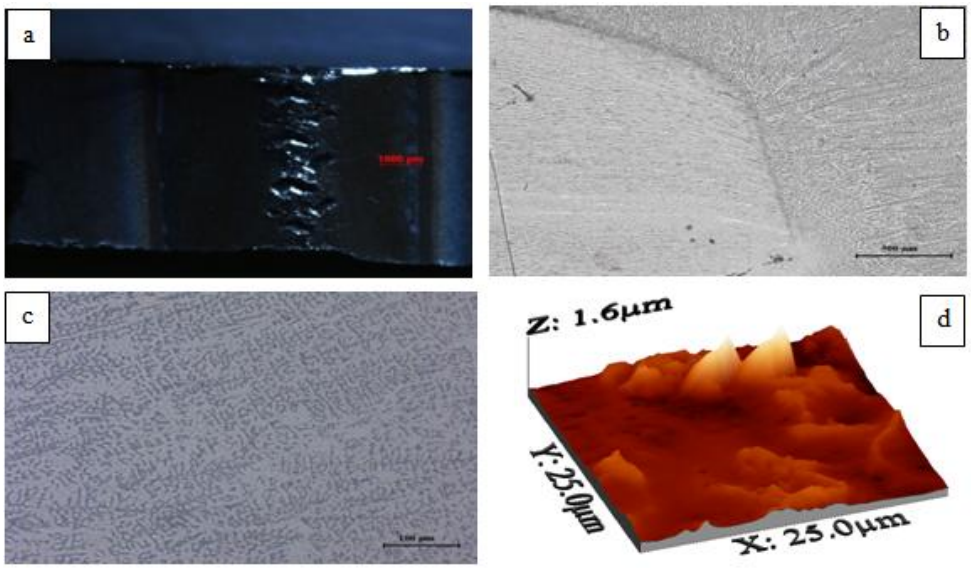

Fig. 4: Surface analysis for CMT weld surface. (a) 5x (b) 50x (c) 200x (d) AFM for 25x25µm^2 surface area

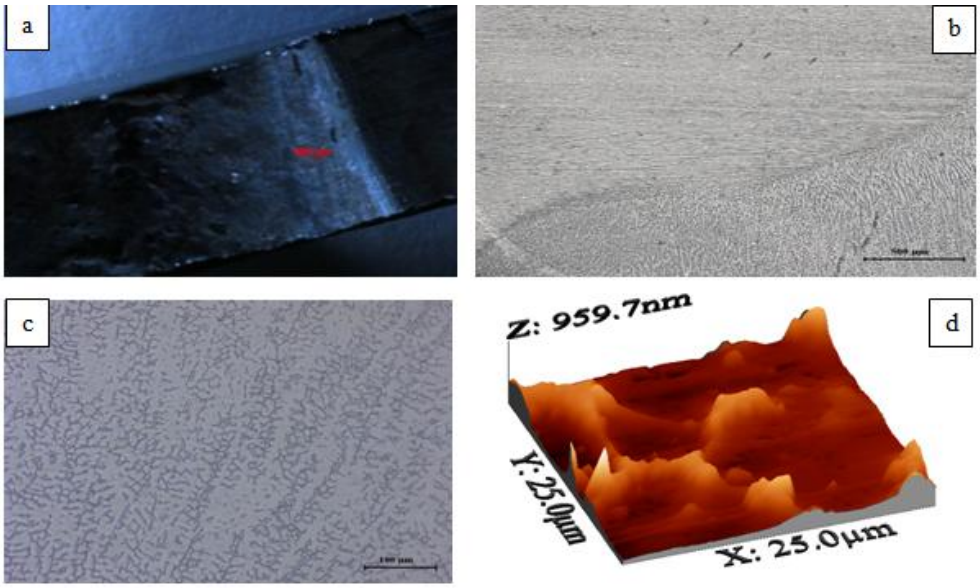

Fig. 5: Surface analysis for MIG weld surface. (a) 5x (b) 50x (c) 200x (d) AFM for 25x25µm^2 surface area

The figures showed that as stainless steel surfaces were welded, the profile become rougher as seen by the increase in peaks. CMT and MIG weld surfaces showed that the surfaces contained mainly peaksand few pits/valleys and suchsurfaces encourage soil film formation. A test was done to determine the bacterial loading and this was compared against R_{max} for the surfaces.The data is presentedbelow.

Table 1: Bacterial loading (*E.coli*)against surface type and maximum height

Surface type	R_{max}(µm)	Average bacterial loading (x10^7)cfu/ml
Normal surface	0.85	79.16±12.64
Laser weld surface	0.83	77.03±14.08
CMT weld surface	1.60	84.80±14.91
MIG weld surface	0.96	143.54±13.14

From the table it was deduced that increase in bacterial loading was from laser weld to normal surface to CMT weld and finally MIG weld. The results were similar to changes in R_{max} for the surfaces which followed the order of laser weld, normal surface, MIG weld and finally CMT weld. These results gave further evidence as

to why welding is prone to MIC as it results in rougher surfaces which attracts more bacteria resulting insoil films.

Surface topography analysis:

Experiments were conducted using 24 kHz ultrasound waves on coupons subjected to 9 adhesion-cleaning cycles. Surface topography was done and the results are presented below, mean and standard deviations were obtained from six sampling positions.

Table 2: Surface topography data(mean±SD)for the different surfaces used in the study

Parameter		Normal surface	Laser weld	CMT weld	MIG weld
	Before	325±4	325±4	325±4	325±4
R_a(nm)	After	192±1	117±2	194±4	148±11
	Change	41%	64%	40%	54%
	Before	395±4	395±4	395±4	395±4
R_q(nm)	After	237±3	155±1	252±3	190±15
	Change	40%	61%	36%	52%
	Before	2.28±0.02	2.28±0.02	2.28±0.02	2.28±0.02
R_{max}x1000 (nm)	After	1.68±0.17	2.00±0.33	1.28±0.02	1.59±0.02
	Change	26%	12%	44%	30%

Increase in R_a before treatment followed the trend LSW⇒NOS⇒CMT⇒MIG and increase in R_a after treatment followed the trend LSW⇒MIG⇒NOS⇒CMT. Significant change in surface topography after treatment with ultrasound waves for all surfaces as seen from % change. Other authors came to the same conclusion that ultrasound wavesresults in smoother surfaces which give better surface cleanability. Other industries make use of ultrasonic electropolishing which yieldfairly uniform, patterned (cratered) surfaces which are attractive forfood and beverage applications [3,20,22,23]. Increase in R_{max} before treatment followed the trend LSW⇒NOS⇒CMT⇒MIG and increase in R_{max} after treatment followed the trend LSW⇒NOS⇒MIG⇒CMT showing asignificant change in R_{max} after treatment with ultrasound waves for all surfaces.

According toDetry*et al.*[3], surface topography of coupons before and after being subjected to ultrasound waves showed that they were comparatively smooth i.e. all R_a values were less than 500nm. High R_a and R_q values before treatment showed that the surface profile could be considered rough as compared to after treatment with ultrasound waves, showing an advantage of ultrasound waves of making the surface smooth during treatment. $R_q$and R_{max}values followed the same trend as R_a for all coupon surfaces.

Surface morphology analysis:

Surface morphology was done for experiments on coupons subjected to 9 adhesion-cleaning cycles and the results are presented below.

Table 3: Surface morphology data(mean±SD) for the different surfaces used in the study

Surface	R_{skw}		R_{kur}		
	Before	After	Before	After	Change
NOS	-0.937±0.001	-0.807±0.037	3.11±0.02	3.28±0.01	(5%)
LSW	-0.937±0.001	0.216±0.056	3.11±0.02	7.47±0.38	(140%)
CMT	-0.937±0.001	0.225±0.020	3.11±0.02	2.23±0.02	28
MIG	-0.937±0.001	0.622±0.020	3.11±0.02	3.58±0.02	(15%)

NOS–normal surface; LSW–laser weld surface; CMT–CMT weld surface; MIG–MIG weld surface

R_{skw} is commonly used to describe the symmetry of the surface while R_{kur} is used to measure the peakedness of the surface, see Appendix I. $R_{skw}< 0$ for normal surface which meant the presence of pits/valleys and this negatively skewed surface was good for lubrication purposes. Welded surfaces had $R_{skw}> 0$ which meant that there was presence of peaks. This data was in agreement and it showed that after welding, the surfaces had peaks giving rougher surfaces i.e. welding processes resulted in surfaces mainly composed of peaks as compared to normal surfaces which are composed of pits/valleys. Small changes in R_{skw} for normal surface showed that there was little effect after use of ultrasound waves i.e. no erosion was experienced. For the welded surfaces, peaks were more pronounced inMIG weld⇒CMT weld⇒Laser weld and this was in agreement with bacterial loading trend as well.

CMT weld surface had $R_{kur}< 3$ which showed lack of high peaks i.e. peaks were greatly eroded during exposure to ultrasound waves and decrease in R_{kur} meant that the surface was flattening during exposure before ultimately forming pits/valleys just like normal surfaces. This process is encouraged as it leads to a smoother surface which is good for lubrication. Normal surface had $R_{kur}\approx 3$ which showed a more even and "smooth" surface and a small change in R_{kur}before and after treatment with ultrasound waves meantthat no erosion was experienced i.e. surface was resistant to ultrasound waves as seen from R_{swk} data. Laser and MIG weld surfaces

had R_{kur}>3 which meant that there was presence of high peaks and increase in R_{kur}observed meant that there surface had more pits than normal surface i.e. weld surfaces were rougher as compared to normal surfaceand this promotes soil film formation. From the data it was also shown that the erosion process was slower on laser and MIG weld surfaces as compared to CMT weld surface.

Surface profile before and after exposure to ultrasound waves:

Analysis before and after treatment was done but only results for normal surface are presented:

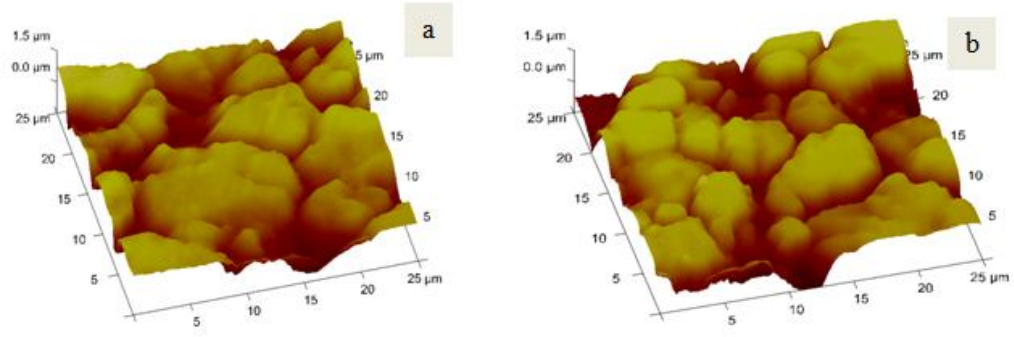

Fig. 6: Change in surface profile for normal surface before and after exposure to ultrasound waves. (a)before treatment and (b) after treatment.

The images revealed that normal surface had an increase in pits/valleys after treatment. Surface with pits/valleys are good for lubrication purposes and the normal surface falls under that category. However, as revealed before, after welding surfaces results in peaks which give poor lubrication conditions.

Discussions:

The observations seen during the study were attributed to implosion of gas bubbles that occurred during cavitation when using ultrasound waves whilst cleaning soil films, leading to erosion of part of the coupon surfaces as observed by[20]for titanium surfaces and[6] for polished steel surfaces. However, erosion is normally not uniform as bubble implosions are never uniform across the surfaces and led to the creation of rougher surfaces that can encourage growth of soil films.

AFM is a non-destructive, practical method for evaluating surface topography and morphology parameters in a quantitative way which has been applied to different coupons in the study. R_a, R_q and R_{max} values of coupons before treatment with ultrasound waves were significantly higher than for coupons after treatment indicating that there was indeed surface erosion i.e. formation of pits and valleys on the coupon surfaces. The deterioration rate was observed on front surfaces which were directly interacting with ultrasound waves and to some extend on the back surfaces not interacting with the waves. The evidence was further supported by R_{skw} values which were below 0 and R_{kur} values above 3 showing deep pits and valleys. Perfect surfaces should have the following characteristics: (i) low bacterial loading, (ii) low R_a, (iii) low R_{max}, (iv)R_{skw} = 0, and (v)R_{kur} = 3. The different surfaces used in the study were ranked from the best to worst according to the results obtained, and they are as follows:

Bacterial loading	Laser weld⇒Normal surface⇒CMT weld⇒MIG weld
R_{max}	Laser weld⇒Normal surface⇒MIG weld⇒CMT weld
R_a and R_q	Laser weld⇒MIG weld⇒Normal surface⇒CMT weld
R_{skw}	Normal surface⇒Laser weld⇒MIG weld⇒CMT weld
R_{kur}	Normal surface⇒CMT weld⇒MIG weld⇒Laser weld

From these observations, three types of surfaces could be defined with respect to surface topography and morphology: (i) polished surfaces where bacteria can be entrapped in grooves as on normal surfaces of coupons used, (ii) pickled surfaces where microorganisms can be entrapped in the grain boundaries as in different welds on coupons or after surface erosion of coupons due to ultrasound waves and (iii) smooth surfaces like glass [19].

Ultrasound waves were found to remove material almost evenly along the coupon surface, thus maintaining the shape of peaks and valleys; however, the erosion occurring during treatment could be controlled and reduced by operating at lower temperatures using pulses in the transport media. These observations can be linked to other authors as well[22].

The relation between the size of the surface defect and the size of microbial cell is important, i.e. microbial cells are retained more by surface defects of similar size as was the case in another study [3]. Grooves larger than the bacteria would behave more like a flat surface while small scratches where bacteria cannot enter will

only reduce the contact area of the cell [3]. *E. coli* cells with lengths of 2–3.4μm and diameters of 0.5–0.9μm on average[24] could settle in grooves or grain boundaries of surfaces used; however, they will be discouraged after significant surface erosion has occurred during treatment. However, regardless of the scale at which roughness is analysed, these measurements are merely statistical values describing a surface, and enable experimental results to be explained only in part. The development of other surface parameters to characterise adhesion is encouraged.

Lastly, surface methods only measured surface residual stresses in one direction and these stresses could be observed only around the weld beam or coupon surface but it does not give any information on the internal material strength [7].

Conclusions:

In the study, the following conclusions were observed:

- Soil films were able to form successfully on stainless steel coupons due to grooves or grain boundaries and on welds used, however, there was greater attachment on the welds due to the thermal stresses than on normal surfaces
- Welding resulted in rougher surface profile which led to increased soil film attachment as observed from R_a, R_{max} and bacterial loading data
- Heat stresses (high temperatures for CMT, Laser and MIG welds) resulted in weaker surfaces which were prone to stress erosion (from ultrasound waves)as observed form R_{skw} and R_{kur} data
- Change in R_{skw} and R_{kur} on welded surfaces showed surface erosion due to the effect of ultrasound waves but it was effective as it enabled chemicals to penetrate the EPS helping to control soil films
- Laser weld gave the best results and it was concluded as the best welding technique but its drawback was on costs as it was an expensive process

ACKNOWLEDGEMENTS

This work is supported by the School of Chemical and Metallurgical Engineering at University of the Witwatersrand, South African Institute of Welding, The Andrew W Mellon Foundation, Biology Department and Falcon Engineering.

Appendices:

Appendix I: Surface topography and surface morphology parameters

1. Average roughness (R_a) – Its widespread use is as a result of its ease of calculation using simple analog devices. Its units of measurement are μm or nm. R_a is the average distance from the profile to the mean line over the length of assessment. R_a does not differentiate between peaks and valleys and is defined as the arithmetic mean of the departure of the surface profile from the mean line. The mean line is a form of reference datum and all the descriptors used to characterise the surface topographies are measured with respect to this line. The mean line is the plane that represents the geometrical plane of the surface where the volumes above and below the plane are equal. R_a values for the test specimens represent the mean departure of the roughness profile from the mean line of the surface. Therefore, the larger the value of R_a, the greater the roughness profile of the surface. It is calculated as:

$$R_a = \frac{\sum_{i=1}^{N} |Z_i - Z_{cp}|}{N}$$

The following image gives a qualitative vision of this parameter:

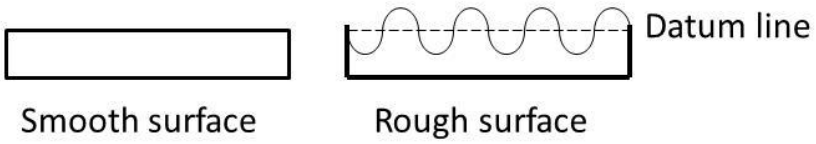

2. Root-mean-square (RMS) profile height (R_q) – This is the square root of the average of the square of the deviation of the profile from the mean line. It is the standard deviation of the Z values within a given area and it is determined by the following formula:

$$RMS = \sqrt{\frac{\sum_{i=1}^{N} (Z_i - Z_{ave})^2}{N}}$$

- Z_{ave} is the average Z value within the given area, Z_i is the current Z value, and N is the number of points within a given area

3. Maximum peak-to-valley height (R_{max})–it is the maximum peak-to-valley height within one cut-off

4. Surface skewness(R_{skw}) – It is a measure of the direction of the asymmetry of thedistribution of heights in the sample or a measure of the average of the first derivative of the surface i.e. the departure of the surface from symmetry. This statistical parameter is given by the following expression:

$$R_{skw} = \frac{\sum_{i=1}^{N}(Z_i - Z_{ave})^3}{N\sigma^3}$$

where $\sigma = \sqrt{\frac{\sum_{i=1}^{N}(Z_i - Z_{ave})^2}{N}}$

The numerical value of R_{skw} gives information about the direction of the asymmetry of thedistribution of heights:

- If $R_{skw}>0$: positive asymmetry(presence of peaks or asperities)
- If $R_{skw}=0$: symmetric distribution(normally distributed surface)
- If $R_{skw}<0$: negative asymmetry(presence of pits or valleys)

5. Surface kurtosis (R_{kur}) – It is a measure of the peakedness of the distribution of heights in the sample by comparing it to the Normal distribution. This statistical parameter is given by the following expression:

$$R_{kur} = \frac{\sum_{i=1}^{N}(Z_i - Z_{ave})^4}{N\sigma^4}$$

where $\sigma = \sqrt{\frac{\sum_{i=1}^{N}(Z_i - Z_{ave})^2}{N}}$

The numerical value of R_{kur} gives us information about the distribution of heights:

- If $R_{kur}>3$: leptokurtic distribution(high peaks or deep valleys)
- If $R_{kur}=3$: mesokurtic distribution(normally distributed surface)
- If $R_{kur}<3$: platykurtic distribution(lack of high peaks or deep valleys)

REFERENCES

[1] Mamvura, T.A., S.E. Iyuke, J.D. Cluett and A.E. Paterson, 2011. Soil films in the beverage industry: A review, Journal of the Institute of Brewing, 117(4): 608-616.
[2] Medilanski, E., K. Kaufmann, L.Y. Wick, O. Wanner and H. Harms, 2002. Influence of the surface topography of stainless steel on bacterial adhesion, Biofouling, 18(3): 193-203.
[3] Detry, J.G., M. Sindic and C. Deroanne, 2010. Hygiene and cleanability: A focus on surfaces, Critical Reviews in Food Science and Nutrition, 50(7): 583-604.
[4] Ramlee, N., M.K. Harun, A. Amrin and A. Ourjini, 2010. Effect of temperature and chloride concentrations on the corrosion behaviour of welded 316L stainless steel, ICFMD, pp: 1-6.
[5] Gandhi, K.S. and R. Kumar, 1994. Sonochemical reaction engineering, Sadhana, 19(6): 1055-1076.
[6] Haosheng, C. and L. Shihan, 2009. Inelastic damages by stress wave on steel surface at the incubation stage of vibration cavitation erosion, Wear, 266(1–2): 69-75.
[7] Uzun, F. and A.N. Bilge, 2010. Investigation of total welding residual stress by using ultrasonic wave velocity variations, Gazi University Journal of Science, 24(1): 43-49.
[8] Antoniadis, A., I. Poulios, E. Nikolakaki and D. Mantzavinos, 2007. Sonochemical disinfection of municipal wastewater, Journal of Hazardous Materials, 146(3): 492-495.
[9] Joyce, E.M, and T.J. Mason, 2008. Sonication used as a biocide, A review: Ultrasound a greener alternative to chemical biocides? Chemistry Today, 26(6): 22-26.
[10] Catallo, W.J. and T. Junk, 1995. Sonochemicaldechlorination of hazardous wastes in aqueous systems, Waste Management, 15(4): 303-309.
[11] Piyasena, P., E. Mohareb and R.C. McKellar, 2003. Inactivation of microbes using ultrasound: a review, International Journal of Food Microbiology, 87(3): 207-216.
[12] Kubo, M., R. Onodera, N. Shibasaki-Kitakawa, K. Tsumoto and T. Yonemoto, 2005. Kinetics of ultrasonic disinfection of Escherichia coli in the presence of titanium dioxide particles, Biotechnology progress, 21(3): 897-901.
[13] Li-xin, B., X. Wei-lin, T. Zhong and L. Nai-wen, 2008. A high speed photographic study of ultrasonic cavitation near rigid boundary, Journal of Hydrodynamics, 20(5): 637-644.
[14] Frantsen, J.E. and T. Mathiesen, 2009. Specifying stainless steel surfaces for the brewery, dairy and pharmaceutical sectors, NACE Corrosion, Paper 09573, Atlanta, USA, 19.
[15] Holah, J.T., 2000. Food processing equipment design and cleanability, Monograph, Flair-Flow Europe technical manual F-FE 377A/00), (Teagasc Organisation), Dublin, p: 47.
[16] Jullien, C., T. Bénezéch, B. Carpentier, V. Lebret and C. Faille, 2003. Identification of surface characteristics relevant to the hygienic status of stainless steel for the food industry, Journal of Food Engineering, 56(1): 77-87.

[17] Vinnichenko, M., Th. Chevolleau, M.T. Pham, L. Poperenko and M.F. Maitz, 2002. Spectroellipsometric, AFM and XPS probing of stainless steel surfaces subjected to biological influences, Applied Surface Science, 201(1): 41-50.
[18] Woodling, S.E. and C.I. Moraru, 2005. Influence of surface topography on the effectiveness of pulsed light treatment for the inactivation of Listeria innocua on stainless-steel surfaces, Journal of Food Science, 70(7): M345-M351.
[19] Boulangé-Petermann, L., R. Rault and M-N. Bellon-Fontaine, 1997. Adhesion of streptococcus thermophilus to stainless steel with different surface topography and roughness, Biofouling: The Journal of Bioadhesion and Biofilm Research, 11(3): 201-216.
[20] Ivanova, E.P., V.K. Truong, H.K. Webb, V.A. Baulin, J.Y. Wang, N. Mohammodi, F. Wang, C. Fluke and R.J. Crawford, 2011.Differential attraction and repulsion of Staphylococcus aureus and Pseudomonas aeruginosa on molecularly smooth titanium films, Scientific Reports, 1(165): 1-8.
[21] Horcas, I., R. Fernandez, J.M. Gomez-Rodriquez, J. Colchero, J. Gomez-Herrero and A.M. Baro, 2007. WSxM: A software for scanning probe microscopy and a tool for nanotechnology, Review of Scientific Instruments, 78: 013705.
[22] Eliaz, N. and O. Nissan, 2007. Innovative processes for electropolishing of medical devices made of stainless steels, Journal of Biomedical Materials Research Part A, 83A(2): 546-557.
[23] Zand, R.Z., K. Verbeken and A. Adriaens, 2012. Electrochemical assessment of the self-healing properties of cerium doped sol-gel coatings on 304L stainless steel substrates, International Journal of Electrochemical Science, 7(10): 9592-9608.
[24] Trueba, F.J. and C.L. Woldringh, 1980. Changes in cell diameter during the division cycle of Escherichia coli, Journal of Bacteriology, 142(3): 869-878.